



MICROCRACK PROPAGATION, COALESCENCE AND SIZE EFFECTS IN COMPRESSION

A. CARPINTERI, C. SCAVIA and G. P. YANG†

Department of Structural Engineering, Politecnico di Torino, 10129, Torino, Italy

Abstract—The strength size effects of brittle materials in compression are studied in the framework of the Boundary Element Method, including the coupling influences of crack interaction, propagation and intersection. Crack interaction coefficients are obtained in the form of algebraic expressions. The curved branching cracks are simulated through a step by step propagation process. Some intersection cracks and edged cracks are checked by the proposed model with acceptable accuracy. With different specimen sizes, crack lengths and proportional crack configurations, the strength size effects are obtained. It is found that the crack interaction, intersection and finite sized boundary have remarkable influence on the loading capacity of the brittle specimen, and that the strength size effects due to crack length and global scaling are not closely connected with the classical stress-singularity power of LEFM. Copyright © 1996 Elsevier Science Ltd.

1. INTRODUCTION

RECENT studies on fracture behaviour of brittle materials help us to interpret the failure mechanism of the structural elements [1, 2]. Among the load-resistant characteristics of brittle materials like concrete and rocks, compressive strength plays a very important role. So far, the complicated behaviour of brittle materials in compression (e.g. the crack interaction, strength size effects, etc.) has not been completely understood.

Brittle failure in compression has been studied theoretically by Nemat-Nasser and Horii [3], in which a closed form solution was obtained for a pre-existing flaw or a regular set of flaws. They assumed that the pre-existing straight crack is closed and the trajectory of the branching crack is straight. Later on, they improved their model to consider the possible curved branching paths [4]. Zaitsev and Wittmann [5] published a paper on crack propagation in compression without consideration of the crack interaction among the distributed cracks in the specimen.

In this paper, crack interaction and propagation, and strength size effects in brittle specimen are studied within the framework of Boundary Element Method by the computer code GEOFF [6, 7]. The fictitious stress elements are adopted to represent the finite sized specimen boundary influence, whereas the displacement discontinuities are used to simulate the effects of the crack in the specimen. The interaction coefficients are obtained in the form of algebraic expressions. Curved branching cracks are simulated through a step by step propagation increment. A special stress element is developed and added to GEOFF to take into account the intersections among cracks themselves and specimen boundaries. Some checking problems of intersection cracks and edged cracks are solved. Comparison between the results from numerical computation and those from referenced analytical solutions shows an acceptable accuracy of the proposed numerical model in simulating various crack geometries. With different specimen sizes, crack lengths and proportional crack configurations, the strength size effects are obtained and discussed.

2. BRIEF DESCRIPTION OF THE DISPLACEMENT DISCONTINUITY METHOD

The Displacement Discontinuity Method (DDM) is based on the assumption that stress and displacement fields are connected with displacement discontinuity (DD) over the crack's two surfaces. Based on the analytical solution of a displacement discontinuity in an elastic field, a crack is subdivided into some elements. The resultant field summing up all the elements' contributions

†On leave from Department of Civil Engineering, Tsinghua University, Beijing, China.

gives out a numerical solution satisfying the given boundary conditions. Usually, the values of the DDs are unknown, but since the tractions applied to the line surfaces are known (e.g. the crack surfaces are stress-free in tension), we can look for the elemental DD necessary to produce these tractions element by element along the crack by solving a system of algebraic equations [8].

2.1. *Stress and displacement field due to a single DD element*

In an infinite field, a DD element takes a portion of length $2a$ on the x -axis (Fig. 1). Constant displacement discontinuities D_x and D_y occur:

$$D_x = u_x(x,0_-) - u_x(x,0_+) \tag{1a}$$

$$D_y = u_y(x,0_-) - u_y(x,0_+) \tag{1b}$$

where u_x and u_y are the displacement components, whose values are taken from the positive side and negative side of the DD element (Fig. 1). These displacements and stresses can be expressed with two functions $f(x,y)$ and $g(x,y)$:

$$\begin{aligned} u_x &= -(1 - 2\nu)f_{,x} - yf_{,xy} + 2(1 - \nu)g_{,y} + yg_{,yy} \\ u_y &= 2(1 - \nu)f_{,y} - yf_{,yy} + (1 - 2\nu)g_{,x} + yg_{,xy} \end{aligned} \tag{2}$$

$$\begin{aligned} \sigma_x &= 2G(f_{,yy} + yf_{,yyy}) + 2G(2g_{,xy} + yg_{,xyy}) \\ \sigma_y &= 2G(f_{,xx} + yf_{,xyx}) + 2Gyg_{,xyx} \\ \sigma_{xy} &= 2Gyf_{,xyy} + 2G(g_{,yy} + yg_{,yyy}), \end{aligned} \tag{3}$$

in which G and ν are the shear modulus and Poisson's ratio, respectively; f , and g , represent the first, second and third order derivatives of functions $f(x,y)$ and $g(x,y)$ with respect to x and y .

Functions $f(x,y)$ and $g(x,y)$ are given by:

$$f(x,y) = \frac{1}{4\pi(1 - \nu)} \int_{-a}^a \hat{u}_y(\eta) \ln[(x - \eta)^2 + y^2]^{1/2} d\eta \tag{4a}$$

$$g(x,y) = \frac{1}{4\pi(1 - \nu)} \int_{-a}^a \hat{u}_x(\eta) \ln[(x - \eta)^2 + y^2]^{1/2} d\eta, \tag{4b}$$

in which $\hat{u}_x(\eta)$ and $\hat{u}_y(\eta)$ are displacement discontinuity distributions on the crack surfaces. In the case of constant displacement discontinuity, the expressions of $f(x,y)$ and $g(x,y)$ can be easily obtained by integral computation, so the stress and displacement field generated by the displacement discontinuities can be evaluated from eqs (2) and (3).

By subdividing each crack into some DD elements, say N elements (Fig. 2), the elemental DDs are defined with respect to local tangential and normal coordinates s and n as D_s and D_n .

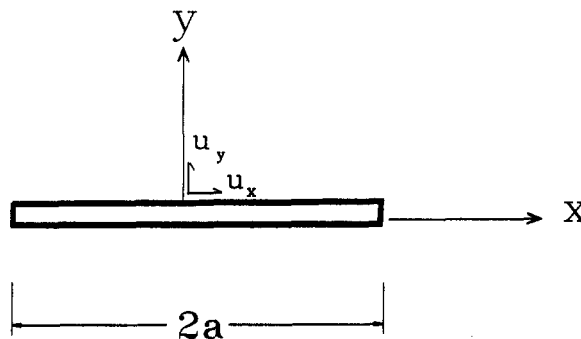


Fig. 1. A displacement discontinuity element.

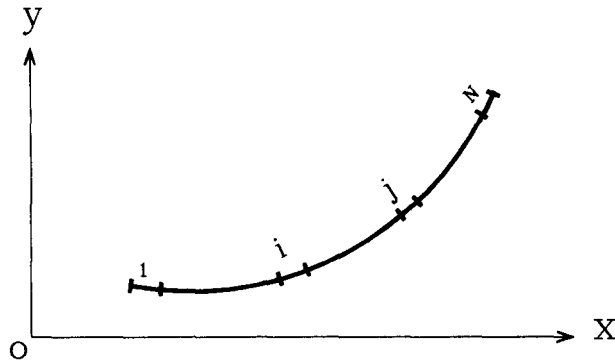


Fig. 2. A crack subdivided into N DD elements.

The resultant stresses and displacements on the position i can be obtained by adding the contributions of all the DD elements:

$$\sigma_s(i) = \sum_{j=1}^N A_{ss}(i,j)D_s(j) + \sum_{j=1}^N A_{sn}(i,j)D_n(j) \tag{5a}$$

$$\sigma_n(i) = \sum_{j=1}^N A_{ns}(i,j)D_s(j) + \sum_{j=1}^N A_{nn}(i,j)D_n(j) \tag{5b}$$

$$u_s(i) = \sum_{j=1}^N B_{ss}(i,j)D_s(j) + \sum_{j=1}^N B_{sn}(i,j)D_n(j) \tag{6a}$$

$$u_n(i) = \sum_{j=1}^N B_{ns}(i,j)D_s(j) + \sum_{j=1}^N B_{nn}(i,j)D_n(j), \tag{6b}$$

in which $A(i,j)$ and $B(i,j)$ are stress and displacement influence coefficients with respect to the displacement discontinuities D_s and D_n , respectively, obtained from eq. (3) suitably modified in order to account for i and j positions.

With the above $2N$ equations, $2N$ unknowns can be obtained by solving these algebraic equations from given boundary stress or displacement conditions, so that the stress and displacement field can be determined. Since the position i can be on cracks or on any other points

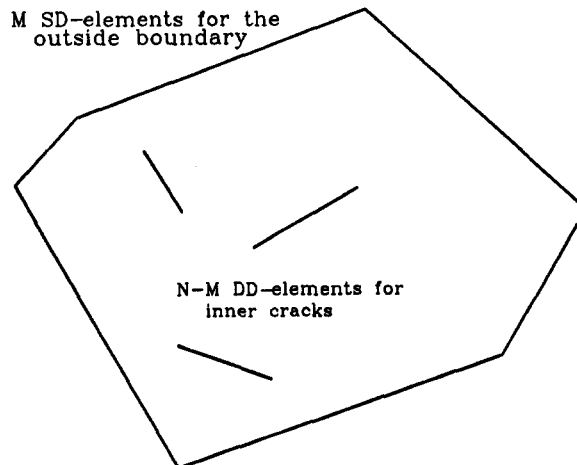


Fig. 3. A finite-sized plate with some inner cracks.

in the specimen, the formulae obtained can be used for computation of the related stress and displacement fields, or for crack interaction effects.

2.2. Fictitious stress elements for external boundary

In the previous section, the formulation procedures are based on the exact solution of crack (displacement discontinuity) in an infinite field. To model the problem with finite sized boundary, Fictitious Stress Method (FSM) is adopted in order to take into account the influence of finite boundary. The formulation of FSM is similar to that of the DDM, so both methods can be hybridized easily.

FSM [8] is based on the exact solution of a point force acting on an infinite plane. A fictitious stress is assumed to act on the discrete boundary element, which is called Stress Discontinuity (SD) element since there exists a stress jump on both sides of the element. Over each element, the stress discontinuities are assumed to vary according to a given mode (constant, linear, etc.), then the stress field generated by M discrete SD elements is:

$$\sigma_s(i) = \sum_{j=1}^M C_{ss}(i,j)P_s(j) + \sum_{j=1}^M C_{sn}(i,j)P_n(j) \quad (7a)$$

$$\sigma_n(i) = \sum_{j=1}^M C_{ns}(i,j)P_s(j) + \sum_{j=1}^M C_{nn}(i,j)P_n(j), \quad (7b)$$

where $P_s(j)$, $P_n(j)$ are the unknown tangential and normal Stress Discontinuities at the mid-point of the boundary elements, $C_{ss}(i,j)$ etc. are the influence coefficients of stresses at point j on those at point i .

In the case of some cracks in a finite body, we can divide the external boundary into M Stress Discontinuity elements and the inner cracks into $N-M$ Displacement Discontinuity elements as shown in Fig. 3.

Thus we can get the following $2N$ algebraic equations:

$$\sigma_s(i) = \sum_{j=1}^M C_{ss}(i,j)P_s(j) + \sum_{j=1}^M C_{sn}(i,j)P_n(j) + \sum_{j=M+1}^N A_{ss}(i,j)D_s(j) + \sum_{j=M+1}^N A_{sn}(i,j)D_n(j) \quad (8a)$$

$$\sigma_n(i) = \sum_{j=1}^M C_{ns}(i,j)P_s(j) + \sum_{j=1}^M C_{nn}(i,j)P_n(j) + \sum_{j=M+1}^N A_{ns}(i,j)D_s(j) + \sum_{j=M+1}^N A_{nn}(i,j)D_n(j), \quad (8b)$$

which enables us to determine the $2N$ unknowns of the SDs and DDs, and then to evaluate the stress and displacement distributions in finite sized plates.

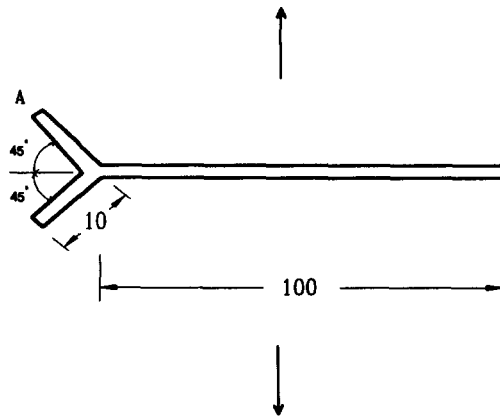
2.3. Determination of stress intensity factors

The Stress Intensity Factors (SIFs) in mixed-mode fracture are directly connected with the displacement discontinuities at the crack tips. Evaluation of the SIFs can be done with known displacement discontinuities at the mid-point of the crack tip element from

$$K_I = D_n G(1 + \nu) \frac{\sqrt{2\pi}}{4\sqrt{r_0}} \quad (9a)$$

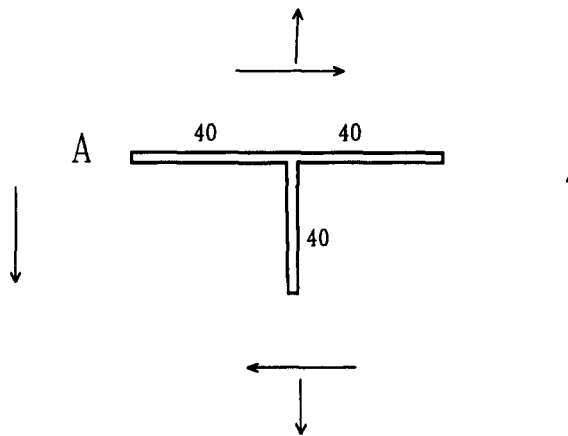
$$K_{II} = D_s G(1 + \nu) \frac{\sqrt{2\pi}}{4\sqrt{r_0}}, \quad (9b)$$

where r_0 is the distance between the crack tip and the point of application of D_s and D_n . It is obvious that the accuracy of the SIF values depends on the accuracy of the displacement evaluation of the



Computed SIF	Reference [10]
$K_{IA} = 73.0811$	72.6353
$K_{IIA} = 43.2156$	44.8630

(4-a)



Computed SIF	Reference [11]
$K_{IA} = 119.9619$	122.1888
$K_{IIA} = 101.1993$	104.3649

(4-b)

Fig. 4. Symmetric branched cracks under plane stress.

crack tips. To improve the solution, a parabolic DD element is used for the crack tip element which makes the evaluation of the SIF more accurate [6, 8].

2.4. Crack propagation simulation

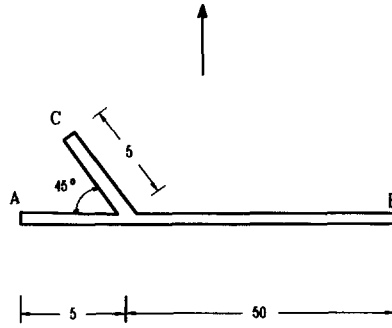
Among candidate criteria of propagation, the Erdogan and Sih criterion [9] has been adopted in this paper. The criterion presents the following form:

$$K_{eq} = \cos \frac{\theta_0}{2} \left[K_I \cos^2 \frac{\theta_0}{2} - \frac{3}{2} K_{II} \sin \theta_0 \right] = K_{IC}, \quad (10)$$

in which K_{eq} is the equivalent stress intensity factor, K_{Ic} is the fracture toughness and propagation angle ϑ_0 satisfies the condition:

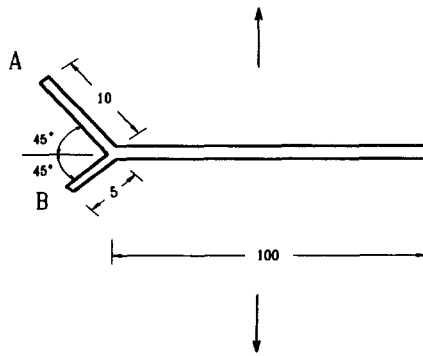
$$K_I \sin \theta_0 + K_{II} (3 \cos \theta_0 - 1) = 0 . \tag{11}$$

Once the propagation condition is met at a crack tip, this tip will start to propagate. For sake of simplicity, the numerical procedures, based on an incremental and iterative load application, will be briefly described below with reference to the propagation of one tip of a single crack [7]. Assume that at the r th step of application of the load, the stress intensity factors K_I and K_{II} have



Computed SIF	Reference [12]
$K_{IA} = 87.5231$	86.6085
$K_{Ic} = 30.6270$	32.7300

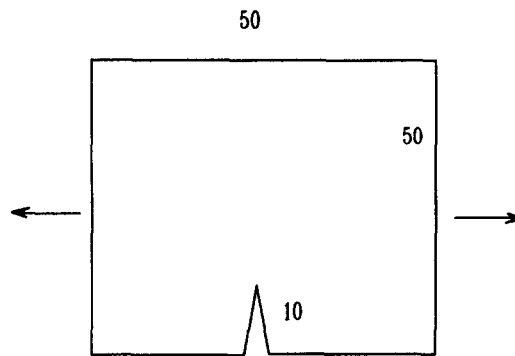
(5-a)



Computed SIF	Reference [10]
$K_{IA} = 82.0164$	81.8927
$K_{IIA} = 56.9197$	57.6809
$K_{IB} = 56.3401$	57.6809
$K_{IIB} = 28.6805$	23.4996

(5-b)

Fig. 5. Asymmetric branched cracks under uniaxial tension.



Computed SIF	Reference [13]
$K_I = 86.8083$	82.9539

Fig. 6. Edged crack under uniform tensile stress.

been computed at one crack tip (say at the m th DD element) and that K_{eq} has been found to be greater than K_{IC} , then

1. a new DD element ($m + 1$) is added at the crack tip m ;
2. the r th load step is repeated with this new crack geometry, and K_{eq} is computed at the new crack tip element ($m + 1$) and compared to the toughness value K_{IC} ;
3. if the value of K_{eq} is smaller than K_{IC} , the next loading step is performed (stable propagation);
4. if the value of K_{eq} exceeds K_{IC} , the load is to be decreased until the propagation condition is met (unstable propagation).

2.5. Crack propagation in compression

The standard DDM described above applies to cracks which are supposed to remain open during the loading process. It does not apply when the crack is in a compressive field:

1. the crack surfaces deform in the normal direction without displacement discontinuities; consequentially, the K_I value is assumed to be zero;
2. if a shear stress is also applied, frictional stresses develop in the tangential direction on the crack surfaces;
3. before maximum shear strength is attained, relative slips of limited magnitude occur between the surfaces of the crack;
4. once maximum shear strength has been attained, relative slips greatly increased, the shear stresses remaining almost equal to maximum shear strength.

So that the DDM has been modified as follows [6].

Normal to the crack, the DDs are assumed to be zero, but the tangential stress acting on the DD element is assumed to increase proportionally to the tangential DDs, and it can increase up to the maximum shear resistance, defined according to Coulomb's failure criterion.

3. CHECKING PROBLEMS ON CRACK INTERSECTION AND EDGE CRACK

In the case of many pre-existing cracks, some branching cracks may intersect each other, so it is necessary to consider the geometry of crack intersection by setting up the intersection criterion, and checking validity of the elements in describing behaviour of the intersection cracks.

The first problem is to set up the criterion for crack intersection. During progressive propagation of cracks in each load step, the new branching crack tip can be in two cases: it crosses

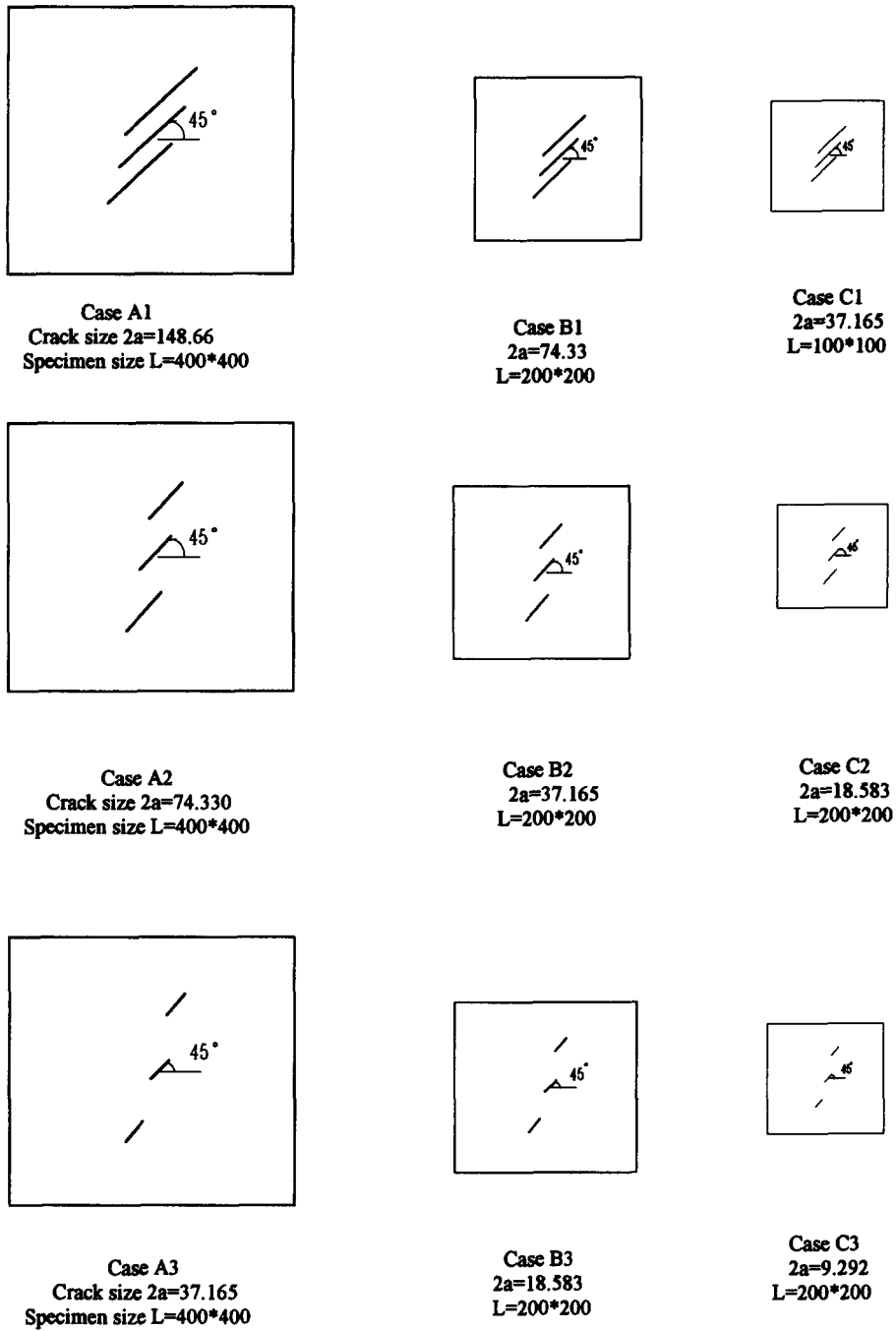


Fig. 7. Nine cases to study strength size effects in compression.

another crack or it approaches another crack within a very small distance. This check is made for the tips of the branching crack in each load step. In both cases, the crack tip is considered to intersect with the corresponding crack element.

Table 1. Compressive stresses of failure for the nine cases of Fig. 7 (N/mm²)

A1	A2	A3	B1	B2	B3	C1	C2	C3
-20	-44	-216	-32	-72	-296	-48	-112	-432

In the former formulations, the displacement discontinuity elements are used to represent the normal cracks without intersection, and the unknowns are the constant displacement discontinuities on each element. However, when two cracks intersect each other, it is difficult to evaluate the displacement discontinuities over these two intersection elements since a new geometric configuration of coalescence cracks is formed. To avoid the difficulty in defining the displacement discontinuities at intersection cracks, a special stress element is formulated to represent the crack intersection, in which the unknowns are the stress distribution on these intersection crack elements.

Taking the fictitious stresses $\hat{\sigma}_y$, $\hat{\sigma}_{xy}$ on the centre of the crack element as unknowns, after getting these stresses, the stress distribution on the crack element is given by

$$\sigma_x(x,0) = \hat{\sigma}_y \frac{-a^2}{x^2 - a^2} \quad (12a)$$

$$\sigma_{xy}(x,0) = \hat{\sigma}_{xy} \frac{-a^2}{x^2 - a^2} \quad (12b)$$

$$\sigma_y(x,0) = \hat{\sigma}_y \frac{-a^2}{x^2 - a^2} \quad (12c)$$

The stress field generated by these crack surface stresses is the same as that of the constant displacement discontinuity over the crack surfaces since the assumed stress distribution on the crack surfaces will make the displacement discontinuities constant. So this stress element is fully harmonized with the formulation procedures in DD element. In the formulation procedures, the interaction coefficients are obtained simply by changing the coefficients and multiplying by some constants.

If crack intersection occurs, the DD element will change to an intersection element which loses the stress singularity at its crack tip and stops propagating. This is because we use continuous stresses on the mid-point position as unknowns, instead of the displacement discontinuities.

To check the validity of the stress element in modelling the intersection behaviour, some problems, for which reference solutions are available, are computed.

Four checking examples are shown in Figs 4 and 5. These examples include symmetric and asymmetric branched cracks under different stress states.

When propagation of the crack reaches the boundary of the specimen, we have an edge crack. The edge crack in a finite width sheet under uniaxial tensile stress without bending constraints is also computed as shown in Fig. 6.

From the above examples, it can be seen that the numerical model proposed in this paper can simulate fracture behaviour of the intersection cracks of complicated geometric shapes with acceptable accuracy.

4. CRACK SIZE EFFECTS

After checking the accuracy of intersection crack problems, we can study the strength size effects of brittle materials with different specimen sizes and different crack lengths, for which the intersection between the cracks will affect the global loading capacity of the specimen.

In the classical Griffith theory of a crack in tension, the crack starts propagating immediately when the SIF achieves the fracture toughness of the material. The propagation is unstable so we usually connect failure load and crack size through the stress singularity $-1/2$. When the problem is finite sized and the crack is in compression, the relation between failure load and crack length presents different characteristics by varying specimen size and/or crack length, because the crack propagation is stable and the crack interaction affects the fracture behaviour. With the aim of studying the strength size effects of the finite sized specimen with different crack length and/or specimen size, we consider nine cases as shown in Fig. 7. The lengths are in mm and the fracture toughness is assumed to be $100 \text{ N/mm}^{3/2}$.

According to these nine cases, two main parameters are varied: crack length and specimen size, as shown in detail in Fig. 7. The failure stresses of these nine cases are shown in Table 1.

Based on the failure stresses outlined above, we will study the influences of crack length and specimen size on the strength of the specimen in two series. The first series is that with the same

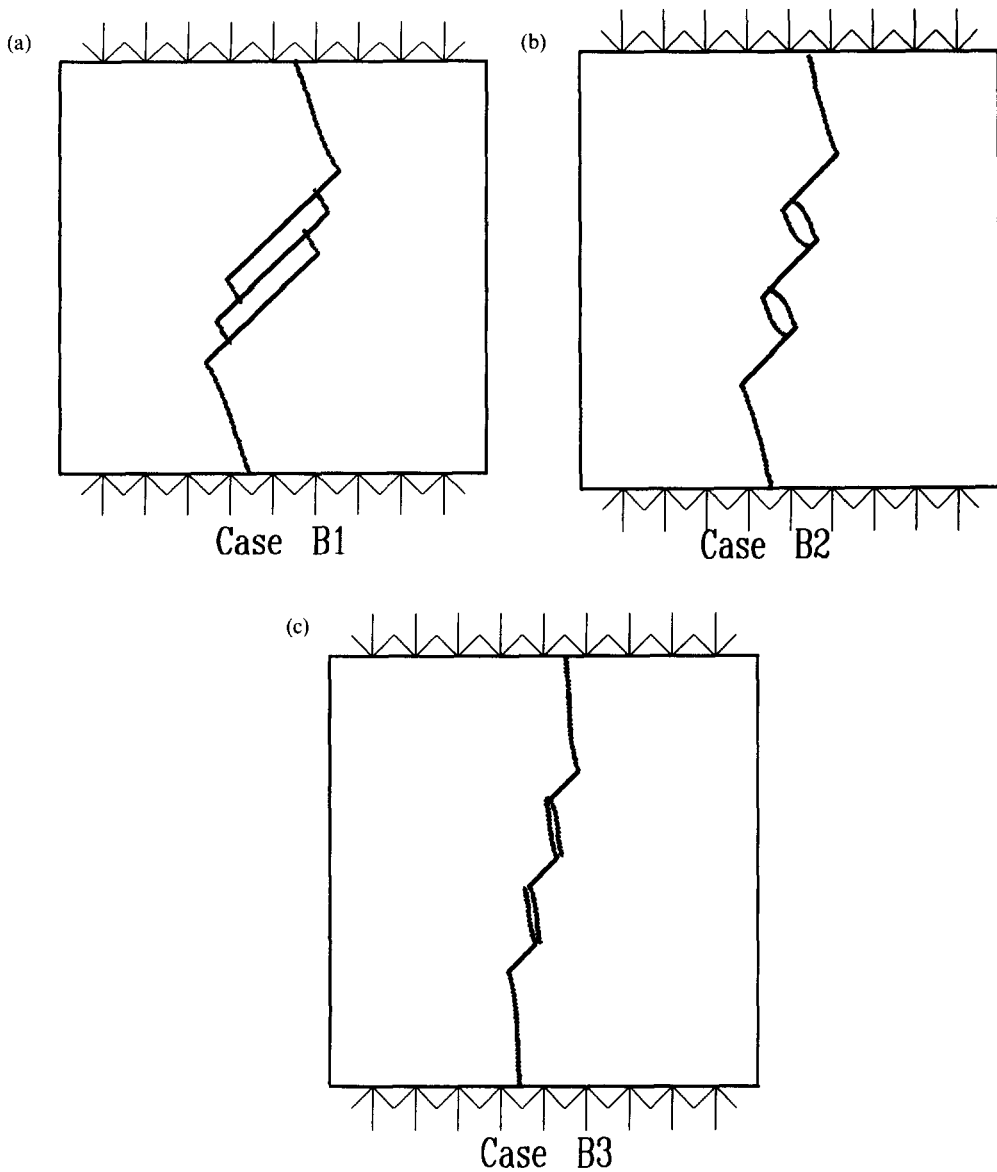


Fig. 8. (a) Final crack pattern of Case B1. (b) Final crack pattern of Case B2. (c) Final crack pattern of Case B3.

specimen sizes but different crack lengths. We have three samples: A1–A2–A3, B1–B2–B3 and C1–C2–C3. With these samples, the influence of the crack length on the loading capacity can be obtained. The final crack patterns in series B1–B2–B3 are shown in Fig. 8(a)–(c), respectively.

In Case B1, branching cracks intersect with primary cracks and then stop propagating, as well as in Case B2. In Case B3, branching cracks do not encounter primary cracks, but they stop propagating due to the strong shielding effects of crack interaction.

The relations between crack lengths and failure stresses are shown in logarithmic form in Fig. 9.

The linear regression equations of these data are respectively:

$$\log \sigma = 4.455 - 1.716 \log a \quad (L = 400)$$

$$\log \sigma = 3.981 - 1.605 \log a \quad (L = 200)$$

$$\log \sigma = 3.656 - 1.585 \log a \quad (L = 100).$$

(13)

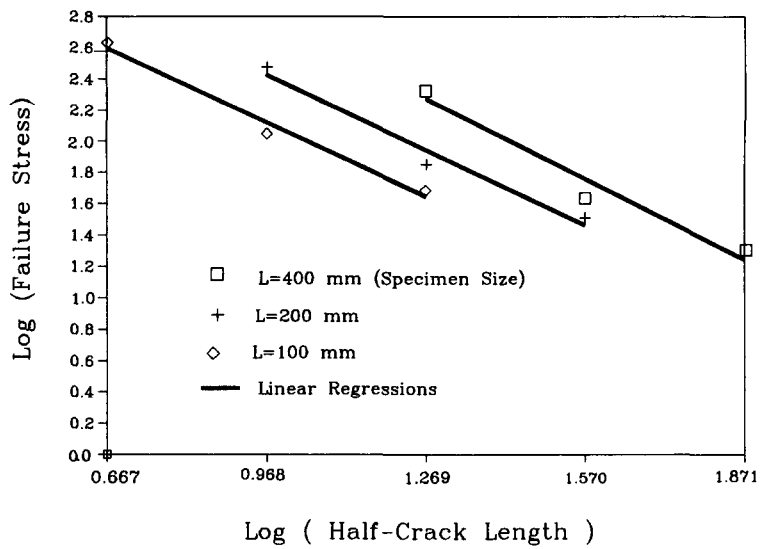


Fig. 9. Relations between failure stress and crack length with constant specimen size.

Equation (13) shows that, in the case of constant specimen size with different crack lengths, the strength size effects related to crack length are given by an absolute slope greater than $3/2$. The failure loads for cracks in compression do not appear connected with the stress singularity $-1/2$ of the Griffith theory since the propagation process in compression is stable, as well as the crack interaction and the finite boundary having remarkable influence on the failure process.

5. SCALE EFFECTS

Let us consider the three groups of samples: A1–B1–C1, A2–B2–C2 and A3–B3–C3. The crack patterns in the final stages of Cases A3 and C3 are shown in Fig. 10(a) and (b), respectively. Together with Case B3 in Fig. 8(c), we can see that the propagation trajectories are very similar in these three cases, although the failure loads turn out to be very different.

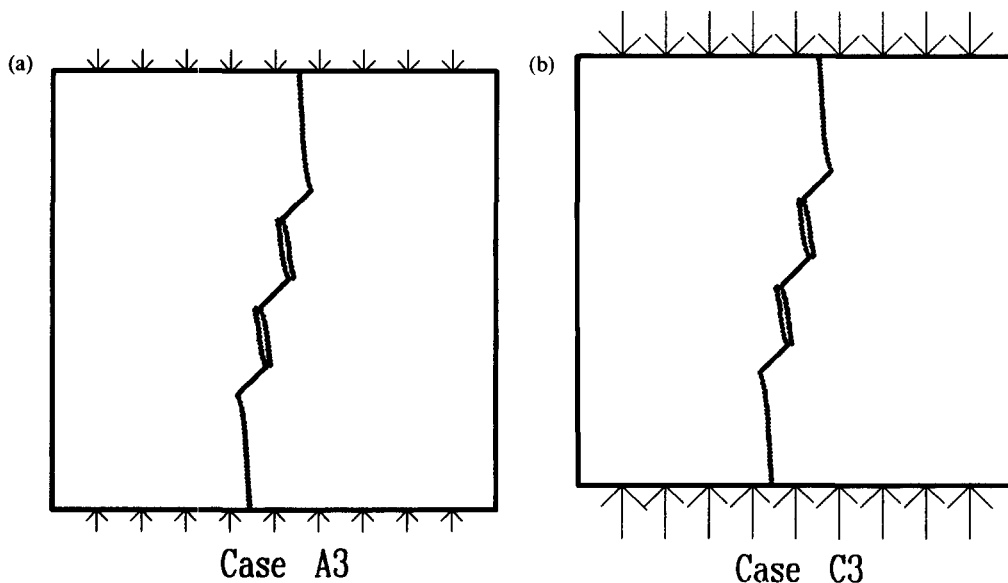


Fig. 10. (a) Final crack pattern of Case A3. (b) Final crack pattern of Case C3.

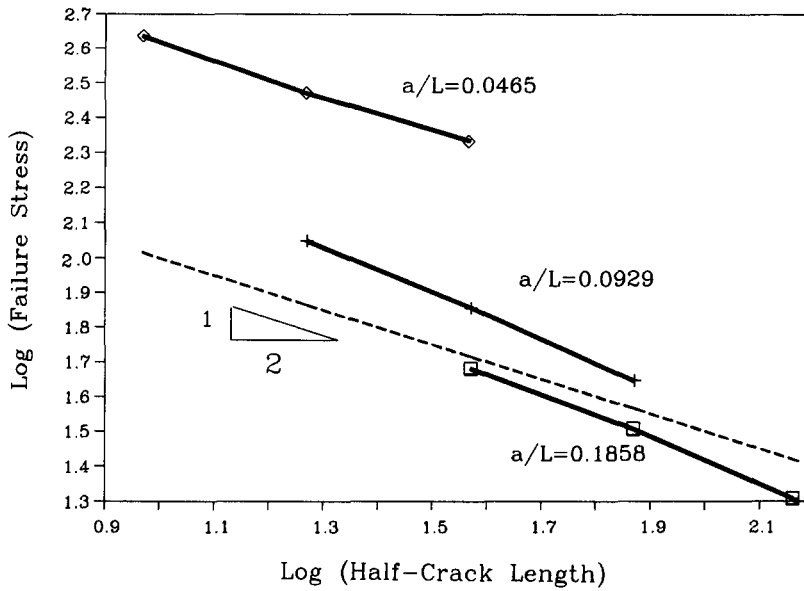


Fig. 11. Relations between failure stress and crack length with global scaling.

The three relations between failure load and crack length, namely A1–B1–C1, A2–B2–C2 and A3–B3–C3, are shown in bilogarithmic form in Fig. 11, in which a line of slope $-1/2$ is also drawn for comparison.

The corresponding linear regression equations are

$$\begin{aligned} \log \sigma &= 2.677 - 0.632 \log a & (a/L = 0.1858) \\ \log \sigma &= 2.908 - 0.674 \log a & (a/L = 0.0929) \\ \log \sigma &= 3.115 - 0.500 \log a & (a/L = 0.0465). \end{aligned} \tag{14}$$

The crack spacings in the above scaling cases are 82.460, 41.230 and 20.615 mm, respectively. To study the influence of crack spacing on strength of the specimen, three additional cases A'1–B'1–C'1 are also computed in which the crack lengths and specimen sizes are the same as those of A1–B1–C1 but the crack spaces are 41.230, 20.615 and 10.308 mm, respectively (half of those in A1–B1–C1). Failure loads are shown in Table 2, in which the values of A1–B1–C1 are again outlined for comparison purpose.

It can be found that the failure stresses with smaller crack spacing are higher than those of larger crack spacing. This is obviously due to the stronger shielding effects from crack interaction corresponding to the smaller spacing.

The linear regression equation for the half crack spacing series A'1–B'1–C'1 is

$$\log \sigma = 2.258 - 0.319 \log a. \tag{15}$$

We should observe that the slopes of the diagrams in bilogarithmic coordinates of eqs (14) and (15), are much less than those of varied crack lengths with constant specimen size of eq. (13). It can be concluded again that, in these cases, the strength size effects are not connected closely with the classical stress singularity $-1/2$ of Griffith theory.

Considering comprehensively the three variables, specimen size L , crack length a and crack spacing d , we can get the multi-variable linear regression for failure stress in compression:

$$\log \sigma = 1.485 + 1.809 \log L - 1.635 \log a - 0.705 \log d. \tag{16}$$

Table 2. Failure stresses with different crack spacings (N/mm²)

A1	A'1	B1	B'1	C1	C'1
-20	-36	-32	-48	-48	-56

From the analysis of the partial derivatives of failure stress with respect to the specimen size, crack length or crack spacing, it can be found that the most important factor is specimen size.

6. CONCLUSIONS

The strength size effects in finite sized brittle specimens in compression are studied in this paper. Some intersection cracks and edge cracks solved by the proposed model are compared with reference solutions. It is found that the crack interaction, intersection and finite sized boundaries have remarkable influence on the loading capacity of the brittle specimens.

From the computations with different specimen sizes, crack lengths and global scaling configurations, the strength size effects are obtained. It can be concluded, from computational results, that in brittle specimens containing cracks in compression the strength size effects due to crack length or global scaling, are not closely connected with the classical stress-singularity $-1/2$ of Griffith theory.

REFERENCES

- [1] A. Carpinteri and A. R. Ingraffea, *Fracture Mechanics of Concrete: Material Characterization and Test*. Martinus Nijhoff (1984).
- [2] *Applications of Fracture Mechanics to Reinforced Concrete* (Edited by A. Carpinteri). Elsevier Applied Science, London (1992).
- [3] S. Nemat-Nasser and H. Horii, Compression-induced non-planar crack extension with application to splitting, exfoliation and rockburst. *J. Geophys. Res. B* **87**, 6805–6821 (1982).
- [4] H. Horii and S. Nemat-Nasser, Compression-induced microcrack growth in brittle solids: axial splitting and shear failure. *J. Geophys. Res. B* **90**, 3105–3125 (1985).
- [5] Y. V. Zaitsev and F. H. Wittmann, Simulation of crack propagation and failure of concrete. *Materials and Structures* **14**, 357–365 (1981).
- [6] C. Scavia, A numerical technique for the analysis of cracks subjected to normal compressive stresses. *Int. J. numer. Meth. Engng* **33**, 929–942 (1992).
- [7] C. Scavia, A method for the study of crack propagation in rock structures. *Geotechnique* **45**, 447–463 (1995).
- [8] S. L. Crouch and A. M. Starfield, *Boundary Element Methods in Solid Mechanics*. George Allen and Unwin, London (1983).
- [9] F. Erdogan and G. C. Sih, On the crack extension in plates under plane loading and transverse shear. *J. bas. Engng, ASME* **85**, 519–527 (1963).
- [10] M. Isida and H. Nohuchi, Formulae of stress intensity factors of branched cracks in plane problems. *Trans. Japan Soc. Mech. Engrs* **49**, 469–479 (1983).
- [11] N. Hasebe and M. Ueda, Crack Originating from a corner of a square hole. *Engng Fracture Mech.* **13**, 913–923 (1980).
- [12] P. S. Theocaris, Asymmetric branching of cracks. *Trans. ASME, Ser. E, J. appl. Mech.* **44**, 611–618 (1977).
- [13] D. P. Rooke and D. J. Cartwright, *Compendium of Stress Intensity Factors*, pp. 84–85. Her Majesty's Stationery Office, London (1976).

(Received 26 December 1994)